

**Minimizing cell number fluctuations in self-renewing tissues with a stem-cell niche**Rutger N. U. Kok , Sander J. Tans,<sup>\*</sup> and Jeroen S. van Zon<sup>†</sup>*Autonomous Matter, AMOLF, Science Park 104, 1098 XG Amsterdam, The Netherlands* (Received 18 November 2022; revised 16 October 2023; accepted 2 November 2023; published 6 December 2023)

Self-renewing tissues require that a constant number of proliferating cells is maintained over time. This maintenance can be ensured at the single-cell level or the population level. Maintenance at the population level leads to fluctuations in the number of proliferating cells over time. Often, it is assumed that those fluctuations can be reduced by increasing the number of asymmetric divisions, i.e., divisions where only one of the daughter cells remains proliferative. Here, we study a model of cell proliferation that incorporates a stem-cell niche of fixed size, and explicitly model the cells inside and outside the niche. We find that in this model, fluctuations are minimized when the difference in growth rate between the niche and the rest of the tissue is maximized and all divisions are symmetric divisions, producing either two proliferating or two nonproliferating daughters. We show that this optimal state leaves visible signatures in clone size distributions and could thus be detected experimentally.

DOI: [10.1103/PhysRevE.108.064403](https://doi.org/10.1103/PhysRevE.108.064403)**I. INTRODUCTION**

Many adult tissues, such as the mammalian intestinal epithelium and the skin epidermis, undergo constant self-renewal supported by stem cells [1,2]. To ensure homeostasis, the number of proliferating cells needs to be kept constant over the lifespan of the organism. Large fluctuations in the number of proliferating cells could lead to disease or even the death of the organism. For that reason, tight regulation of cell proliferation is required [3–5], where every cell division must result in one proliferating and one nonproliferating cell, at least on average.

The balance of proliferation and differentiation can either be maintained strictly at the single-cell level or at the population level [6]. In the first strategy, every cell division produces an asymmetric outcome: one daughter cell remains proliferative and the other daughter ceases proliferation and terminally differentiates. In the population level strategy, the outcome of each division is stochastic and can result in zero, one, or two proliferating daughters. In this case, the balance between proliferation and terminal differentiation is maintained only on average, at the population level [7]. This maintenance strategy is therefore called the population-asymmetry model.

Unlike the single-cell level strategy, the population level strategy is inherently stochastic and therefore potentially prone to fluctuations in the number of proliferating cells. Despite these fluctuations, the population level strategy of self-renewal is found in many stem-cell systems [3]. Examples

include the mammalian germline, the intestine, and the epidermis [6,8–11]. In some organs, large variations of the number of stem cells can occur, such as for spermatogenic stem cells in murine testes [7]. As such fluctuations are potentially dangerous, in other organs the number of stem cells appears to be tightly controlled, such as in the small intestine [12]. It is unknown how different strategies of stem-cell maintenance affect fluctuations in stem-cell numbers.

In many stem-cell systems, cell proliferation is also organized in space, with stem-cell niches that provide a local environment that maintains stem cells in an undifferentiated and proliferating state [7], while cells outside of such stem-cell niches eventually cease proliferation and differentiate. As a consequence, the division patterns of proliferating cells also likely vary in space, with more divisions generating proliferating cells within the stem-cell niche, and more nonproliferating cells without. How such a spatial segregation of proliferation dynamics might impact fluctuations in cell proliferation remains an open question.

Here, we use a theoretical approach to study the impact of different stem-cell maintenance strategies, including whether or not a stem-cell niche is present, on fluctuations in the number of proliferating cells. In particular, we compare proliferation dynamics in a uniform, unbounded system, i.e., lacking a stem-cell niche, and a system with two compartments, i.e., a stem-cell niche where cells are geared towards proliferation, and a differentiation compartment where cells are biased towards ceasing proliferation. We analytically derive under which conditions the two-compartment model is stable, meaning that the number of proliferating cells is stationary, and calculate the corresponding steady-state number of proliferating cells. We then systematically examine how different parameters, such as the fraction of symmetric and asymmetric division or the size of the stem-cell niche, impact the magnitude of fluctuations. We find that in the uniform model, fluctuations are minimized when all divisions are asymmetric, strictly generating one proliferating and one

<sup>\*</sup>tans@amolf.nl<sup>†</sup>j.v.zon@amolf.nl

*Published by the American Physical Society under the terms of the Creative Commons Attribution 4.0 International license. Further distribution of this work must maintain attribution to the author(s) and the published article's title, journal citation, and DOI.*

nonproliferating daughter. Surprisingly, we find that in the two-compartment model, that incorporates a stem-cell niche, fluctuations are instead minimized by a very different strategy: when all divisions are strictly symmetric, generating either two proliferating or two nonproliferating daughters. Finally, our simulations show that these different strategies generate distinct clone size distributions and could thus potentially be differentiated experimentally [5].

## II. RELATED WORK

Theoretical models have advanced our understanding of stem-cell behavior. These models have focused on two main questions. First, what is the impact of various niche setups on cell number fluctuations? And second, what is the role of (a)symmetry in cell divisions [4,5]?

We will first discuss the impact of niche setup on cell number fluctuations. The models used to study fluctuations can roughly be divided into three classes. A first class of models uses a uniform space with two cell types: proliferating and nonproliferating. Klein *et al.* [13] used such a model to determine the impact of various division strategies on the fluctuations of cell numbers, but only for individual lineages. Sun and Komarova [14] used the same type of model to test the impact of various feedback mechanisms on cell number fluctuations. Those feedback mechanisms required that cells are aware of the current amount of stem cells in the system. However, it is open question whether such feedback mechanisms are present in stem-cell systems.

A second class of models uses a single compartment with a fixed number of stem cells, and no other cell types. These models were used to study competition between lineages. Snippert *et al.* [10] and Lopez-Garcia *et al.* [9] demonstrated that the intestinal crypt uses neutral competition, where the progeny of one stem cell eventually takes over the entire niche. Ritsma *et al.* [11] and Corominas-Murtra [15] studied the dependence of lineage survival on cell position within the niche.

Finally, in a third class of models, two cell types (stem and nonstem) are distributed over two compartments. In this work, we will use a model of this class. So far, these models have only been used to study the risk of developing cancer, namely, by Cannataro *et al.* [16,17] and Shahriyari and Komarova [18]. Therefore, the question of how a compartmentalized system affect fluctuations in the number of cells remains open.

The second question is about the impact of division symmetry. The studies that focused on this question so far used a model with uniform space and both proliferating and nonproliferating cells. Klein *et al.* [13] used this model to infer division symmetry from experimental data of the skin epidermis and concluded that asymmetric divisions were dominant. Sei *et al.* [19] used a similar setup for the intestinal crypt, and likewise concluded that asymmetric divisions were dominant. Yang and Komarova [20] used the model for a different purpose: they investigated the impact of division symmetry on fluctuations in the number of proliferating cells. The authors found that their results were mixed. Under some control mechanisms, symmetric divisions provide lower fluctuations, but under most control mechanisms, asymmetric divisions

provide lower fluctuations. Therefore, it remains unclear what impact division symmetry has on the fluctuations in cell numbers.

## III. ONE-COMPARTMENT MODEL

We start our analysis by looking at a model without space, corresponding to Klein *et al.* [13]. In the next section, this model will be extended to include a niche compartment. We use two cell types: proliferating and nonproliferating. Whether or not a cell is proliferative is decided at the birth of the cell; this fate cannot be changed later. Every proliferating cell will divide  $T$  hours after the birth of the cell, while nonproliferating cells will never divide. Values of  $T$  are drawn from a skew-normal distribution [21] with a skewness parameter 6.1, a location of 12.2, and a scale of 5.3. This distribution approximates cell cycle times we recently measured in intestinal organoid crypts [22].

After a division, two daughter cells are created, which can be (I) both proliferating, (II) both nonproliferating, or (III) one can be proliferating and the other nonproliferating [Fig. 1(a)]. The chances for these division types to occur are  $p$ ,  $q$ , and  $1 - p - q$ , respectively. Division types I and II are symmetric, while type III is asymmetric. The values of  $p$  and  $q$  are determined by two parameters. The parameter  $\phi = p + q$  is the chance of a division being symmetric [Fig. 1(b)], while the other parameter, the growth rate  $\alpha = p - q$ , is the average increase in the number of proliferating cells per division [Fig. 1(c)]. One can verify that for  $\phi = 0$ , all divisions are required to be of type III, while for  $\alpha = 1$ , all divisions are required to be of type I.

For homeostasis, in this system it is required that the growth rate  $\alpha = 0$ . For  $\alpha > 0$ , the number of proliferating cells would grow exponentially, and for  $\alpha < 0$ , this number would decrease exponentially. The symmetry fraction  $\phi$  can be varied freely, as well as the initial number of proliferating cells,  $D$ . We therefore perform a simulation for different combinations of  $D$  and  $\phi$ , while keeping  $\alpha$  at 0. The results are displayed in Figs. 1(d)–1(g).

In Fig. 1(d), six simulations of the number of proliferating cells are shown over time for two values of the symmetry fraction  $\phi$ . We can observe that a higher fraction of asymmetric divisions (low  $\phi$ ) provides a system with less fluctuations in the number of proliferating cells. In addition, we see that the system with a high fraction of symmetric divisions (high  $\phi$ ) is frequently depleted of proliferating cells, while the smaller system with a high fraction of asymmetric divisions (low  $\phi$ ) remains stable for at least 10 days. In Figs. 1(e)–1(g), the depletion rate, overgrowth rate, and coefficient of variation in the number of proliferating cells are plotted as a function of both the initial number of proliferating cells,  $D$ , and the symmetry fraction  $\phi$ . Here, depletion is defined as the number of proliferating cells becoming zero, while overgrowth is defined as the number of proliferating cells reaching five times the initial amount. We can see that the depletion and overgrowth rates increase for smaller  $D$  and larger  $\phi$ , indicating a less stable system. The coefficient of variation remains high irrespective of  $D$  and  $\phi$ , with one exception: the theoretical case where precisely all cell divisions are asymmetric ( $\phi = 0$ ), the coefficient is zero.

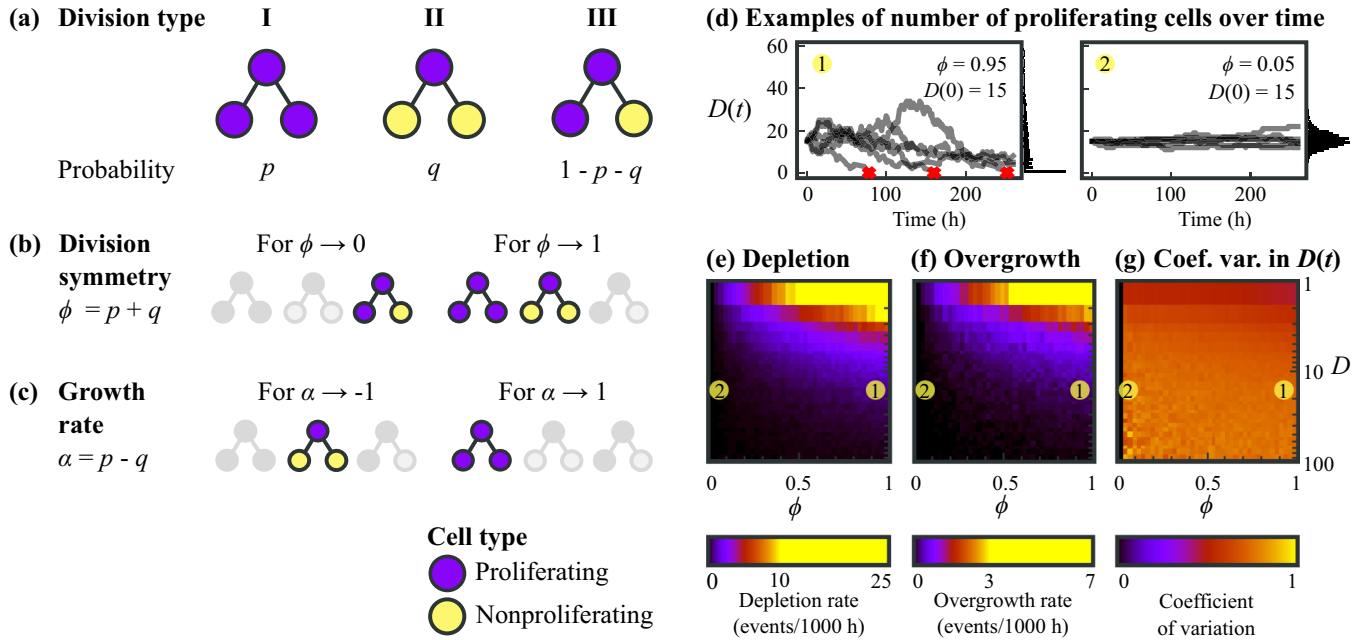


FIG. 1. The uniform model. (a) All possible division types and their probability. (b) Dominant division type for two different division symmetries. (c) Dominant division type for two different growth rates. (d) Number of proliferating cells over time, for simulations with initial condition  $D(0) = 15$  and different symmetry fraction  $\phi$ . Lines indicate six individual simulations, while the histograms represent the distribution of proliferating cells after 260 hours, for 2000 simulations. Red markers indicate events where proliferating cells were fully depleted. (e) Depletion rate, the rate of how often the number of proliferating cells drops to zero. (f) Overgrowth rate, the rate of how often the number of proliferating cells grew larger than five times the initial number of proliferating cells. (g) Coefficient of variation of the number of dividing cells. In (e)–(g), the values for each parameter set were calculated over  $10^5$  hours total simulation time.

As a result, in this model, the best approach to minimize fluctuations and avoid depletion or overgrowth of proliferating cells would be to have a large number of proliferating cells and to use strictly asymmetric divisions. A low amount of symmetric divisions already results in relatively large fluctuations in the number of proliferating cells.

IV. TWO-COMPARTMENT MODEL

We wanted to compare the performance of the uniform model, in terms of the impact of fluctuations, to a model that incorporated a stem-cell niche. We therefore constructed a different model, that included two compartments, with cell proliferation differing between compartments. One compartment, which we call the niche compartment, can only contain a fixed number of cells. In contrast, the other compartment, which we call the differentiation compartment, is unbounded in size. This two-compartment model is sketched in Fig. 2.

The niche compartment is set to contain a fixed number of cells in total, denoted as  $S$ . Of this number, a variable number of cells,  $N(t)$ , is proliferative, which makes the number of nonproliferating cells equal to  $S - N(t)$ . For the differentiation compartment, we denote the number of proliferating cells as  $M(t)$ . As the differentiation compartment is unbounded in size, we do not keep track of the number of nonproliferating cells in this compartment. The total number of proliferating cells over both compartments is defined as  $D(t) = N(t) + M(t)$ . To keep the niche compartment fixed in size, upon every division in the niche compartment, we move one random cell out of the niche compartment into the

differentiation compartment. Instead of a single growth rate  $\alpha$ , both compartments can now have different growth rates. We define the niche compartment as having a growth rate  $\alpha_n$  and the differentiation compartment as having a growth rate  $\alpha_m$ . For simplicity, for now we assume that the division symmetry fraction  $\phi$  is the same for both compartments.

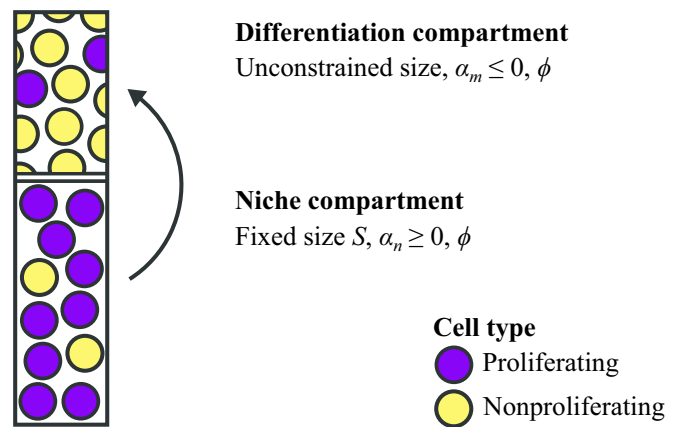


FIG. 2. Illustration of the two-compartment model. Two compartments are defined: the niche compartment and the differentiation compartment. In the niche compartment, the growth rate  $\alpha_n \geq 0$ , while in the differentiation compartment, the growth rate  $\alpha_m \leq 0$ . The fraction of symmetric divisions  $\phi$  is equal in both compartments. Upon a division in the niche compartment, one random cell moves from the niche compartment to the differentiation compartment.

A challenge in comparing fluctuations in the number of proliferating cells,  $D(t)$ , between different parameter sets is that varying parameters completely independently will cause changes in the average cell number  $\langle D(t) \rangle$ . Increasing the average cell number by itself will already decrease fluctuations, obscuring the impact on fluctuations that is purely due to differences in the cell proliferation strategy. It is therefore important to vary parameters in a concerted manner, which ensures that the average number of proliferating cells remains unchanged. To find an expression that relates the number of proliferating cells to the underlying parameters, we first examined a deterministic version of the two-compartment model.

## V. SOLUTION OF THE DETERMINISTIC TWO-COMPARTMENT MODEL

In the two-compartment model, cell proliferation in the differentiation compartment only occurs through cells ejected from the niche compartment and their offspring. Ejection of a cell from the niche compartment in turn requires cell division within the niche compartment. As a consequence, the influx of proliferating cells in the differentiation compartment strongly depends on the rate of cell divisions in the niche compartment, and thus on the parameters  $\alpha_n$ ,  $\phi$ , and  $T$ . To explicitly take into account cell cycle progression, we used a transport model, arriving at the following two equations for the niche compartment:

$$\frac{\partial n(t, a)}{\partial t} + \frac{\partial n(t, a)}{\partial a} = -\frac{n(t, T)}{S}n(t, a), \quad (1)$$

$$n(t, 0) = (1 + \alpha_n)n(t, T). \quad (2)$$

The full derivation can be found in Appendix. In the above equations,  $a$  is the age of a cell, with  $a = 0$  for newly born cells, and  $a = T$  at the moment of a cell division.  $n(t, a)$  is the average number of cells at a given time with a given age, and integrating over all values of  $a$  results in  $N(t)$ , the average number of proliferating cells in the niche compartment. The transport model describes the number of cells of age  $a$  to  $a + da$  at time  $t$ . This number changes due to cell cycle progression, cell divisions, and proliferating cells exiting the niche compartment. At every cell division, on average,  $1 + \alpha_n$  proliferating daughters are born. In addition, exactly one cell is ejected from the niche compartment, which has a chance of  $\frac{N(t)}{S}$  of being a proliferating cell.

For the differentiation compartment, we arrive at a transport equation [Eq. (A5)] that resembles Eq. (1), but with a positive right-hand term representing the influx of cells from the niche compartment. In the steady state, we arrive at the following solution for the average number of dividing cells in both compartments:

$$D = \ln(1 + \alpha_n)S \frac{\alpha_m - \alpha_n}{\alpha_m}. \quad (3)$$

This equation depends on the parameters  $\alpha_n$  and  $\alpha_m$  in a nontrivial manner. At the same time, it matches an intuitive understanding of the key properties of the two-component model. First,  $D > 0$  requires  $\alpha_m < 0$  and  $\alpha_n > 0$ , meaning that the growth rate of the niche compartment is positive and the growth rate of the differentiation compartment is negative. For other values, the systems either decays or grows without

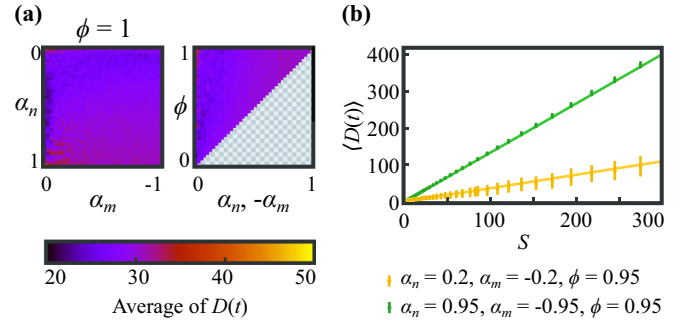


FIG. 3. (a) Average of  $D(t)$  for a  $10^5$  h simulations of each parameter set. Niche size  $S$  was set according to Eq. (3) so that on average, the total number of dividing cells was  $D = 30$ , as confirmed by the simulations. The figure uses the same layout as Fig. 4(b). (b) Average value  $\langle D(t) \rangle$  (markers) as a function of niche size  $S$  for different values of the other model parameters. Error bars are standard deviation. Lines show  $D$  calculated using the deterministic model in Eq. (3).

bounds. Second,  $D$  increases with increasing values of  $\alpha_n$  and  $\alpha_m$ . In particular,  $D = 0$  independent of  $\alpha_m$  for  $\alpha_n = 0$ , while  $D$  increases well beyond the niche size  $S$  for  $\alpha_m \approx 0$ .

At the same time, Eq. (3) also provides insights that are less intuitive. First, despite the key role of cell divisions in the niche compartment, whose rate depends on  $T$  and  $\phi$ , these parameters do not enter the steady-state expression for  $D$ . Second, even though the link between the niche and differentiation compartments, through division-driven ejection of cells from one to the other, is potentially complex, Eq. (3) finds that the dependence of the number of proliferating cells is comparatively simple, with  $D$  showing a simple linear dependence on niche size  $S$ .

## VI. STOCHASTIC SIMULATIONS OF THE TWO-COMPARTMENT MODEL

### A. Impact of fluctuations

Building on the above analytical results of the deterministic two-compartment model, we then examined the sensitivity of the stochastic two-compartment model to fluctuations. For a uniform system, asymmetric divisions resulted in a system with smaller fluctuations in the number of proliferating cells. We therefore specifically examined if more division asymmetry also results in smaller fluctuations in the two-compartment model.

We first confirmed that the average behavior of the stochastic model indeed reproduced the predictions in Eq. (3) [Fig. 3(a)]. Next, we performed a parameter sweep, sampling all possible combinations of  $\alpha_n$ ,  $\alpha_m$ , and  $\phi$ , while keeping the initial number of proliferating cells at  $D = 30$ . Here, we used Eq. (3) to calculate the niche size  $S$  required to achieve this, meaning that  $S$  varied with  $\alpha_n$  and  $\alpha_m$ . In addition, cell cycle times were determined as outlined in Sec. III. We reproduced the expected average value  $\langle D(t) \rangle = 30$  for all combinations of  $\phi$ ,  $\alpha_n$ , and  $\alpha_m$  [Fig. 3(b)], confirming again the validity of our analytical result in Eq. (3).

In Fig. 4(a), we show  $D(t)$  for two parameter sets that strongly differ in the degree of symmetry. In the first case,

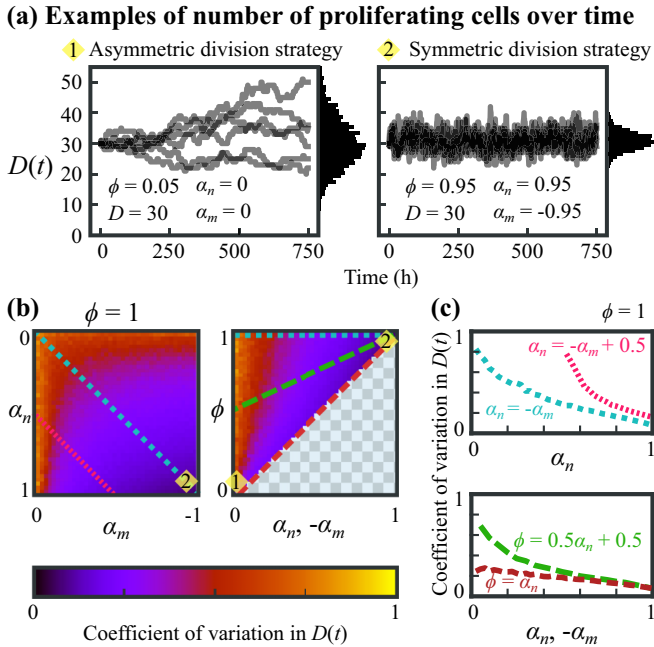


FIG. 4. Exploration of the two-compartment model. Niche compartment size  $S$  is set according to Eq. (3) so that the average number of proliferating cells is set to  $D = 30$ . (a) Two panels showing  $D(t)$  for six example simulations each of the optimal parameters for either an asymmetric division strategy (left) or a symmetric division strategy (right). Simulations ran for 750 hours. Histograms show distribution of  $D$  at the simulation end point for 2000 simulations. (b) Overview of the coefficient of variation in the number of dividing cells,  $D(t)$ . The blocked areas represent impossible combinations of parameters, such as strictly asymmetric divisions with a positive growth rate. For each parameter set, values were calculated over  $10^5$  hours total simulation time. (c) Coefficient of variation along selected lines. Line style matches the lines of (b).

almost all cells divide asymmetrically, while  $\alpha_n, \alpha_m = 0$ , thus corresponding to the strategy that minimizes fluctuations in the uniform model. In the second, all cells divide symmetrically, while the growth rate strongly differs between compartments. Interestingly, we find that the parameter set with a high fraction of symmetric divisions results in smaller fluctuations in  $D(t)$ . This is in contrast to the uniform model, where asymmetric divisions always provided less fluctuations compared to symmetric divisions.

In Fig. 4(b), we quantify the coefficient of variation in  $D(t)$  for different combinations of  $\alpha_n$ ,  $\alpha_m$ , and  $\phi$ . In general, we find that fluctuations decrease when the difference in growth rate between compartment,  $\alpha_n - \alpha_m$ , increases. When we focus on the subset of parameter sets with  $\alpha_n = -\alpha_m$ , we find that for a fixed value of the two growth rates, fluctuations are reduced by increasing the fraction of asymmetric divisions (decreasing  $\phi$ ), which appears consistent with our results for the uniform model and at odd with our observation in Fig. 4(a) that high symmetry resulted in low fluctuations.

To examine this further, we compare in Fig. 4(c) the coefficient of variation along the four lines shown in Fig. 4(b). In the top panel, we compare two lines for parameter sets with only symmetric divisions ( $\phi = 1$ ) that have either a larger (cyan)

or smaller (pink) difference in growth rate between the two compartments. In both cases, the coefficient of variation in  $D(t)$  decreases with increasing difference in growth rates, but the parameter sets with the smaller difference (pink) always showed larger fluctuations.

The bottom panel shows two other lines, where we are varying  $\phi$  while fixing  $\alpha_n = -\alpha_m$ . The red line uses, for every value of  $\alpha_n$ , the lowest possible value of  $\phi$ , i.e., the maximum amount of asymmetry that the growth rate permits. At  $\alpha_n = 1$ , all divisions are symmetric. The green line has a higher fraction of symmetric divisions. The lines show that for a given growth rate  $\alpha_n$ , the parameter set with the highest asymmetry results in the smallest coefficient of variation in  $D(t)$ , as seen above. However, at the same time, the global minimum of the coefficient of variation is found for  $\alpha_n, -\alpha_m = 1$ . This is because the decrease in fluctuations is strongest when the difference in the two growth rates is maximal. For these values of the growth rate, only  $\phi = 1$  is allowed, which is a system with only symmetric divisions. Therefore, although asymmetry generally reduces the coefficient of variation in  $D(t)$ , the optimal solution is a fully symmetrically dividing system.

In Fig. 4, we assumed, for simplicity, that the symmetry fraction  $\phi$  was equal for both compartments. We examined whether our conclusions were impacted by allowing the niche and differentiation compartments to have distinct symmetry fractions:  $\phi_n$  and  $\phi_m$ , respectively. Overall, we found that that increasing  $\phi_m$  increased fluctuations in the number of dividing cells, although this impact was typically small compared to that of increasing  $\phi_n$  [Figs. 5(a) and 5(b)]. For sufficiently high  $\phi_n$  and depending on the value of the other model parameters, fluctuations in  $D(t)$  could, in principle, be lowered by decreasing  $\phi_m$  relative to  $\phi_n$ . However, overall fluctuations were minimized for  $\alpha_n, -\alpha_m = 1$  and  $\phi_n, \phi_m = 1$  [Fig. 5(c)], corresponding exactly to the global minimum identified in Fig. 4. Overall, this shows that allowing  $\phi$  to differ between compartments did not enable division strategies with even lower fluctuations than the optimal strategy we already identified.

Overall, we conclude that in the two-compartment model, the best strategy to minimize fluctuations in the number of proliferating cells,  $D(t)$ , is to use a system where all cells in the niche compartment proliferate, but each cell born outside the niche compartment immediately stops proliferating. This results in the dominance of symmetric cell divisions. Other solutions, such as strictly asymmetric divisions or a combination of symmetric and asymmetric divisions, result in more fluctuations in the number of proliferating cells.

## B. Dependence of fluctuations on niche size

Next, we wondered what the influence of the size of the niche compartment would be on the stability of the system. For each size, we plot the coefficient of the variation along two lines. For the first line, we take the line that describes all points for which  $\phi = \alpha_n, -\alpha_m$ , corresponding to the red dashed line in Fig. 4(b). This is the line with the lowest coefficient of variability in the number of dividing cells,  $D(t)$ , for every  $\phi$ . For the second line, we examine the dependence of the niche compartment size  $S$  for the parameters on the line with  $\phi = 1$  and  $\alpha_n = -\alpha_n$ , corresponding to the cyan dotted

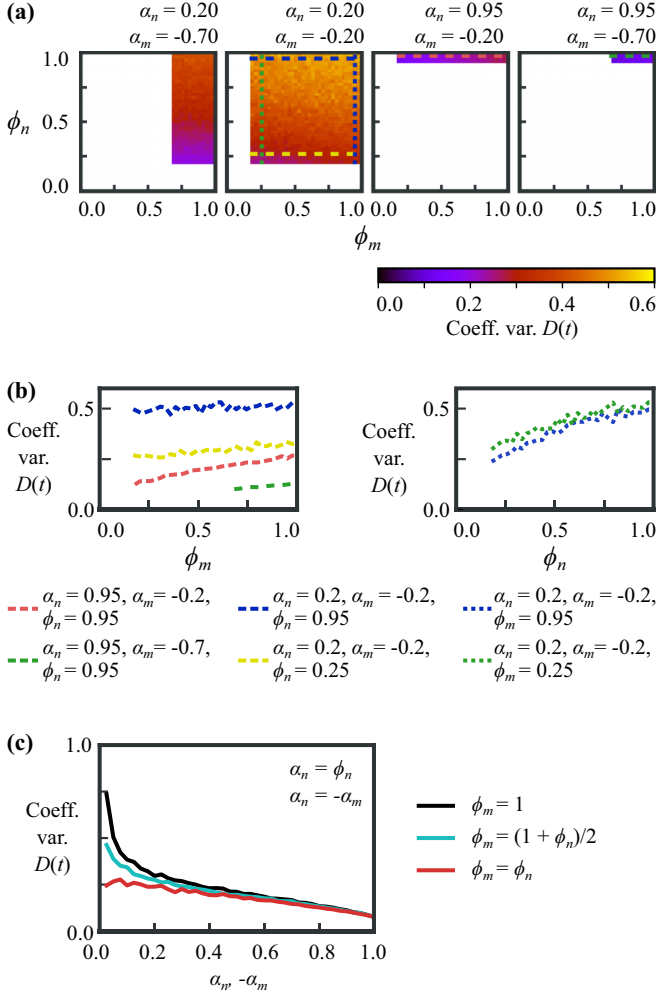


FIG. 5. Impact of different values of  $\phi_n$  and  $\phi_m$  for the niche and differentiation compartment, respectively. (a) For each value of  $\phi_n$  and  $\phi_m$ , one simulation of  $10^5$  hours was performed. Part of the simulation space is inaccessible (indicated by the white region), as  $\phi_n$  can never be smaller than  $\alpha_n$ , and  $\phi_m$  never smaller than  $|\alpha_m|$ .  $S$  was chosen such that  $D = 30$  in Eq. (3). Shown is the impact of varying  $\phi_n$  and  $\phi_m$  on the coefficient of variation of  $D(t)$ , for different combinations of  $\alpha_n$  and  $\alpha_m$ . (b) Coefficient of variation in  $D(t)$  along the lines show in (a). Overall, the variation in  $D$  increases with  $\phi_m$ , i.e., more symmetric divisions in the differentiation compartment. However, this impact is small compared to that of increasing  $\phi_n$ . (c) Coefficient of variation in  $D(t)$  when increasing  $\phi_m$  for  $\alpha_n, -\alpha_m = \phi_n$ . The red line, with  $\phi_n = \phi_m$ , corresponds to the red line in Figs. 4(b) and 4(c) and represents the parameter sets that minimize fluctuations in  $D$  for the given  $\alpha_n$ . Here, increasing  $\phi_m$  raises fluctuations in  $D$ , in particular for low  $\alpha_n$ . Fluctuations are minimized for  $\alpha_n, -\alpha_m = \phi_n, \phi_m = 1$ , corresponding to the global minimum found in Fig. 4

line in Fig. 4(b). This line represents the line with the largest difference in coefficient of variability of  $D(t)$ ; it goes from the global minimum to the global maximum of the coefficient of variability in  $D(t)$  for a given  $S$ .

The results are displayed in Fig. 6(a). Consistent with the results above, for every given size, increasing the difference in growth rates  $\alpha_n$  and  $\alpha_m$  will always result in a system with

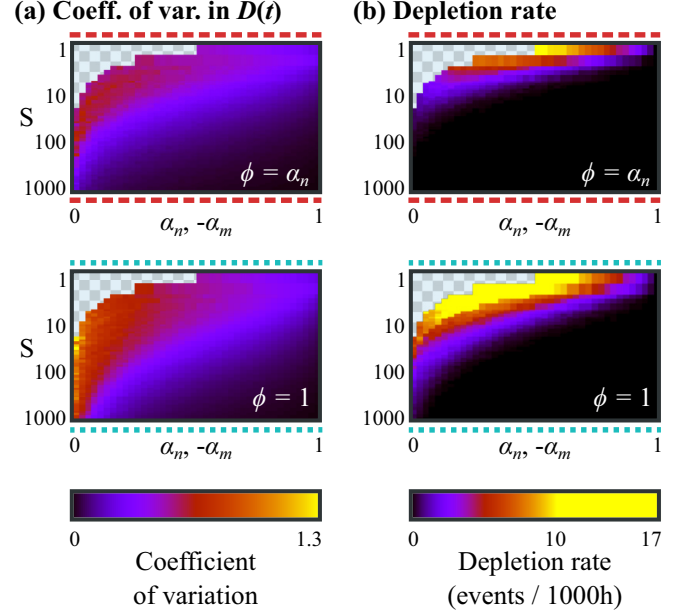


FIG. 6. Simulations for different niche compartment sizes  $S$ , each for  $10^5$  hours. The initial number of dividing cells,  $D$ , is set according to Eq. (3). The striped lines above and below the graphs correspond to the lines in Fig. 4. The blocked areas in the graphs are parameter ranges for which Eq. (3) does not give a solution. (a) Coefficient of variation of  $D(t)$  for various parameters. (b) Depletion rate for various parameters.

a lower coefficient of variation in  $D(t)$  and a lower depletion rate. Moreover, at larger compartment sizes  $S$ , the coefficient of variation in  $D(t)$  always becomes lower. Therefore, independent of the chosen parameter set, a system can always decrease its relative fluctuations by creating a larger niche. For the same reason, decreasing the niche compartment size results in more frequent depletions of the proliferating cells [Fig. 6(b)].

The observation that a smaller system results in more fluctuations is as expected. However, interestingly even for small niche sizes, the system can remain stable, provided the symmetry fraction is high. Decreasing the niche compartment size from  $S = 30$  to only  $S = 10$  still results in a system with low fluctuations (less than 1 collapse per 10 years), provided the niche compartment maintains a high growth rate and symmetry fraction.

### C. Determining growth rate and division symmetry by clone size distributions

Experiments often measure clone size distributions using lineage tracing. For instance, using a model analogous to the uniform model above, the division symmetry  $\phi$  was estimated by fitting to experimental long-term clone size scaling distributions, measured for different time frames [13]. We therefore asked whether parameters such as growth rate and division symmetry could also be inferred from clone size distributions obtained in the context of the two-compartment system.

For short-term clone size distributions, the dominance of symmetric divisions appears clearly as an enrichment of even

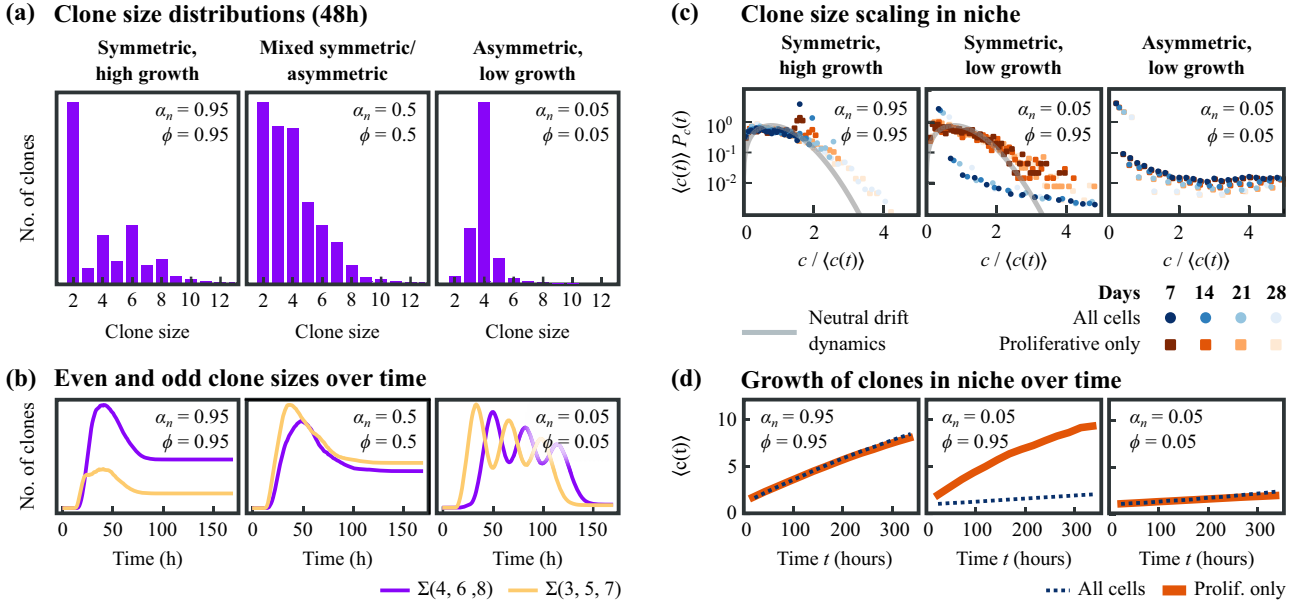


FIG. 7. Clone size distributions of cells within the niche compartment. 1000 simulations per parameter set,  $\alpha_m = -\alpha_n$ ,  $D = 30$ , and  $S$  is set according to Eq. (3). (a) Short-term clone size distributions, taken after 40 hours. (b) Amounts of even and odd clone sizes over time. For the symmetric, high-growth case, there is initially a large enrichment of even clone sizes, which becomes smaller after 50 hours. For the mixed symmetric-asymmetric case, odd clone sizes are enriched. For the asymmetric case, all clones grow at almost the same rate, and therefore a single clone size is dominant at any point in time. This causes oscillatory behavior in whether even or odd clone sizes are dominant. (c) Clone size scaling for the symmetric, low-growth case. For these parameters, there is a large contrast between the clone size distribution of all cells and the clone size distribution of only the proliferating cells. (d) Growth of the average clone size over time.

clone sizes. In Fig. 7(a), we show simulated clone size distributions of 1000 simulation runs, taken after 48 hours. For the case where symmetric divisions are dominant [ $\phi = 0.95$ , displayed in Fig. 7(a), left], we can see that even clone sizes 2, 4, 6, and 8 all occur in higher frequencies than the odd clone sizes 3, 5, and 7. This enrichment is not visible for systems where asymmetric divisions are dominant or where neither division type is dominant [Fig. 7(a), center and right].

However, as the clone size over time in Fig. 7(b) shows, this enrichment of even clone sizes is strongest until 60 hours. In addition, during the entire simulation, the enrichment is barely visible for clone sizes larger than 8 [Fig. 7(a) and Fig. 8]. In the simulation, this has two causes. First, we simulate for  $\phi = 0.95$ , which still results in 5% of all divisions being asymmetric. While symmetric divisions will keep the clone size of a single lineage even, asymmetric divisions will not. Already a single asymmetric division anywhere in the lineage tree results in the clone size becoming odd.

Second, the variability in cell cycle times also contributes to the occurrences of odd clone sizes. Consider, for example, two proliferating sister cells. Initially, the clone size is two, and after both sisters have divided, it is four. However, in between the divisions of both sisters, the clone size is three and therefore odd. This effect occurs more often for large lineage trees, simply because there are more sister pairs, therefore increasing the chance of at least one of them making the clone size odd. In conclusion, the effect of division symmetry is visible only on the timescale of a few divisions.

Often, clone size growth is characterized experimentally by the clone size scaling function  $P_c(t)$  [5], which is a function that gives the probability of finding a clone of size  $c$  at

time  $t$ . Unlike the distributions discussed above, the scaling function  $P_c(t)$  is not dependent on time, but only on the clone size divided by the average clone size for that time:  $P_c(t) = f(c/\langle c(t) \rangle)$ . Would there be a way to measure both the symmetry fraction and the growth rate from this scaling function? In other words, do the symmetry fraction and growth rate affect the observed long-time scaling behavior?

In experiments, clone size distributions are often collected only in the stem-cell niche. Moreover, our simulations do

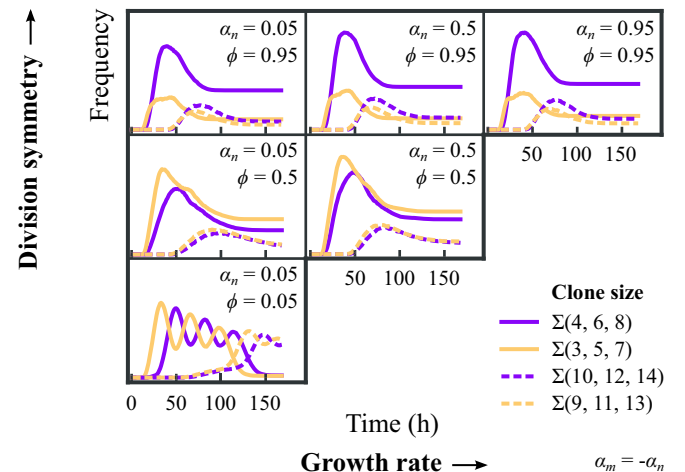


FIG. 8. Clone sizes plotted over time for the entire system, for the sums of the given even and odd clone sizes. The evolution of the clone size depends mainly on the division symmetry, not on the growth rate. Each parameter set consists of 1000 simulations.

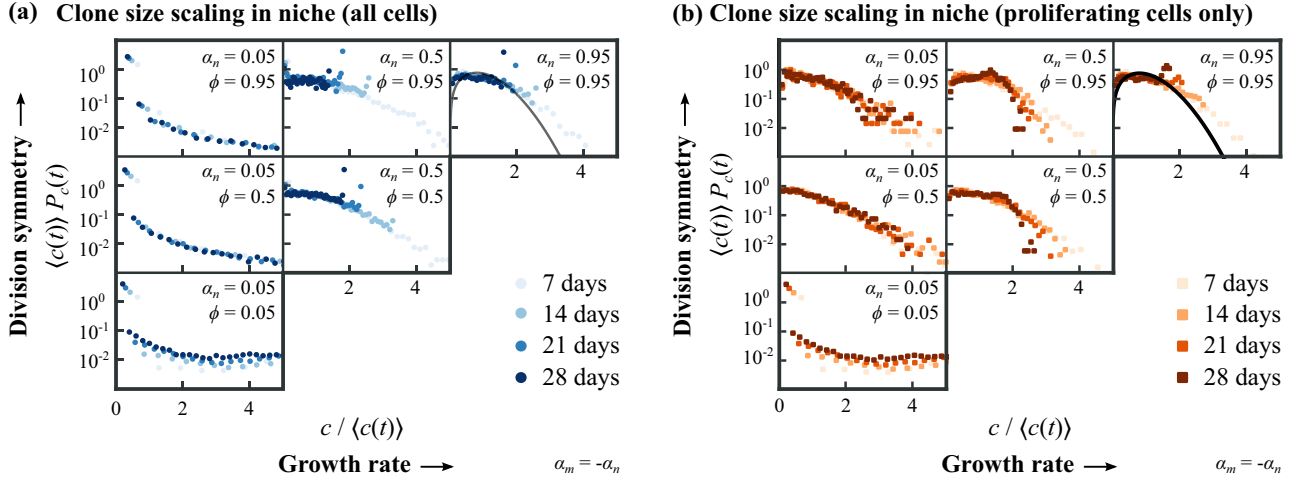


FIG. 9. Scaling function for various configurations. Each parameter set consists of 1000 simulations. (a) Scaling functions that include all cells in the niche compartment. (b) Scaling functions that include only the proliferating cells in the niche compartment.

not implement cell death, which results in the number of nonproliferating cells outside the niche compartment growing continuously. Such unbounded growth would prevent any long-term scaling behavior. For that reason, we will, in our analysis, ignore all cells outside the niche compartment.

We calculated the scaling function of different combinations of the symmetry fraction  $\phi$  and growth rate  $\alpha_n$ . First, we find that for all parameters examined, the clone size distributions scale, meaning that they fall on the same curve independent of time, both when considering only proliferating cells or all cells in the niche compartment. In Fig. 7(c), we show the scaling functions, both for all cells in the niche compartment and for only the proliferating cells. Interestingly, the shape of the scaling function for the proliferating cells in the niche is almost independent of the growth factor  $\alpha_n$ , as both for  $\alpha_n = 0.05$  [Fig. 7(c), left] and  $\alpha_n = 0.95$  [Fig. 7(c), center] the scaling function follows a concave shape. Instead, the scaling function for proliferative cells depends on the symmetry fraction  $\phi$ : for high-symmetry fractions, the scaling function follows the concave pattern predicted by neutral drift dynamics [9], which is  $\langle c(t) \rangle P_c(t) = (\pi x/2) e^{-\pi x^2/4}$ , with  $x = c/\langle c(t) \rangle$  [Fig. 7(c), left and center], while for low-symmetry fractions, the scaling function follows a convex shape [Fig. 7(c), right].

However, if we look at all cells in the niche, including nonproliferating cells, then the scaling function no longer depends on the symmetry fraction  $\phi$ , but on the niche growth rate  $\alpha_n$ . For high  $\alpha_n$ , the scaling function follows a concave shape [Fig. 7(c), left], while for low  $\alpha_n$ , the function follows a convex shape [Fig. 7(c), center and right]. The scaling functions of other parameter sets are displayed in Fig. 9 and are consistent with these observations.

The cause of this scaling behavior can be seen in Fig. 7(d). In this panel, we plot the average clone size over time for the same three parameter sets. As expected, the average clone size for all cells in the niche compartment increases faster for a high growth rate [Fig. 7(d), left] compared to a low growth rate [Fig. 7(d), center and right]. However, if we include only the proliferating cells, then the clone size growth depends on

$\phi$ . For high  $\phi$  [Fig. 7(d), left and center], the clones grow faster than for low  $\phi$  [Fig. 7(d), right]. This is because the number of proliferating cells can only grow due to symmetric divisions, as asymmetric divisions do not have an effect on the number of proliferating cells. Even though the total number of proliferating cells is independent of  $\phi$  [Eq. (3)], the proliferating cells are now distributed over more clones. We can see that the fast-growing clones in Fig. 7(d) correspond to the concave scaling functions in Fig. 7(c), and the slow-growing clones correspond to the convex scaling functions.

## VII. DISCUSSION

In this paper, we investigated the impact of fluctuations for different stem-cell maintenance strategies, in the context of a stem-cell niche. For this, we used a model with two compartments and two cell types, namely, proliferating cells and nonproliferating cells. The model assumes a stem-cell niche that is restricted in size, and in which cells decide whether or not to continue proliferating depending only on the basis of the identity of the compartment in which they are born. No other interactions between cells are assumed, and besides their proliferation state, no other internal cellular state is considered. The key parameters governing the dynamics of this model are each compartment's growth rate, which indicates how many proliferating cells are produced on average through each cell division, and the division symmetry, that describes how likely two daughter cells are to have the same proliferating or nonproliferating cell type.

We used a transport model approach to obtain an analytical solution describing the average dynamics of the two-compartment model. Combined with stochastic simulations, we found that this model allowed for two distinct strategies to minimize stem-cell number fluctuations under homeostatic conditions. If the two compartments do not differ in growth rate, then the overall growth rate must be zero to balance proliferation and cells must maximize the fraction of asymmetric divisions. This special case of our model corresponds to the one-compartment model previously developed by Klein *et al.*

[13], and also used by Sei *et al.* [19]. However, if the two compartments are allowed to differ in growth rate, then another strategy is possible that exhibits substantially lower cell number fluctuations. In this strategy, fluctuations are minimized when the difference in growth rate between the two compartments is maximized and hence all divisions are symmetric. This finding is in contrast to the view that asymmetric divisions offer a more regulated stem-cell maintenance process in stem-cell niches [23,24], but consistent with measurements recently performed by us that show that symmetric divisions dominate in growing intestinal organoids [22]. In this optimal limit, the dynamics in the niche compartment of our model becomes similar to the models of Snippert *et al.* [10] and Lopez-Garcia *et al.* [9]. Our results thus show that their models, which were based on experimental observations, correspond to a parameter regime, in our more general model, that minimizes fluctuations in the number of proliferating cells.

Our simulations indicate that the key parameters of our model, i.e., growth rate and division symmetry, can be determined experimentally through measuring clone size distributions. Clone size distributions are commonly measured using techniques such as genetic lineage tracing [25,26]. For sufficiently short times (0–50 hr, corresponding to a few cell cycles) high division symmetry can be detected through enrichment of even-sized clones. Indeed, we recently observed such an enrichment in intestinal crypts *in vivo* using lineage tracing [22], in agreement with the high division symmetry that we observed in intestinal organoids by direct cell tracking. However, for most experiments, clone size distributions are collected over much longer timescales, for which our simulations show that enrichment of even-sized clones is no longer observable. Here, we found that growth rate and division symmetry can still be determined by comparing clone size distributions either for all cells in the stem-cell niche or only proliferating cells, as they give rise to different scaling functions for clone size distributions as well as distinct increases in average clone size. Experimentally, this could be readily achieved by combining lineage tracing reporters with antibody markers for cell proliferation.

Many stem-cell systems share the two-compartment architecture of the intestine, with a small niche containing stem cells that inject differentiating cells into the rest of the tissue [27]. It will therefore be interesting to experimentally test whether such tissues also exhibit dynamics consistent with the optimal limit of our model, with a strong difference in growth rate between the stem-cell niche and the rest of the tissue, and most divisions symmetric, producing either two proliferating or two nonproliferating daughters. Our analysis provides a starting point to test this experimentally.

#### ACKNOWLEDGMENTS

We would like to thank M. A. Betjes for useful discussions, suggestions, and comments. R.K. was funded by an NWO Building Blocks of Life grant from the Dutch Research Council, Grant No. 737.016.009.

#### APPENDIX: DERIVATION OF EQ. (3)

When a cell is born, it is set to be either proliferating or nonproliferating. Proliferating cells will divide  $T$  hours after

they are born, while nonproliferating cells will not divide. Here,  $T$  is a normal distribution. We define  $n(t, a)da$  as the number of proliferating cells in the niche compartment at time  $t$  with age bracket  $(a, a + da)$ . Here, age is defined as the time since the last division. The number of cells flowing in and out of this age bracket due to aging is

$$J_+ = \frac{dt}{da} n(t, a - da) da,$$

$$J_- = -\frac{dt}{da} n(t, a) da.$$

The rates for cells entering and exiting the niche compartment are defined as  $k_+(a)$  and  $k_-(a)$ , respectively. Note that in our simulation, cells do not reenter the niche compartment so  $k_+(a) = 0$ .

Using this information, we look at how the number of cells of a particular age bracket evolves over time. This number is equal to the number of existing cells of that age bracket, plus the number of incoming cells due to aging, minus the number of cells exiting the age bracket due to aging, plus the number of cell changes due to cells entering and exiting the compartment:

$$n(t + dt, a) da = n(t, a) da + \frac{dt}{da} n(t, a - da) da - \frac{dt}{da} n(t, a) da + (k_+(a) + k_-(a)) da dt.$$

Rearranging, we find

$$\frac{n(t + dt, a) - n(t, a)}{dt} + \frac{n(t, a) - n(t, a - da)}{da} = k_+(a) + k_-(a).$$

Using the definition of the derivative, we readily find

$$\frac{\partial n(t, a)}{\partial t} + \frac{\partial n(t, a)}{\partial a} = k_+(a) - k_-(a). \quad (\text{A1})$$

#### 1. Growth boundary condition

Next, we introduce the growth boundary condition. If there are no cells moving in between compartments, then  $k_+(a) = k_-(a) = 0$  and  $dN = J_{\text{in}} - J_{\text{out}}$ . Here,  $J_{\text{out}} = \frac{dt}{da} n(t, T) da$  is the rate of cells exiting the cell cycle, and  $J_{\text{in}}$  is the rate of cells entering the cell cycle. As each division produces, on average,  $\alpha + 1$  proliferating cells,  $J_{\text{in}} = (\alpha + 1) J_{\text{out}}$ . Together,

$$\frac{dN}{dt} = \frac{J_{\text{in}} - J_{\text{out}}}{dt} = \alpha n(t, T). \quad (\text{A2})$$

From the definition  $N(t) = \int_0^T da n(t, a)$ , it follows that

$$\frac{dN}{dt} = \int_0^T da \frac{\partial n(t, a)}{\partial t}.$$

From Eq. (A1) in the case where  $k_+(a) = k_-(a) = 0$ , we can see that  $\frac{\partial n(t, a)}{\partial t} = -\frac{\partial n(t, a)}{\partial a}$ . Inserting this into the above integral and evaluating it results in

$$\frac{dN}{dt} = n(t, 0) - n(t, T). \quad (\text{A3})$$

Combining Eq. (A3) with Eq. (A2) results in

$$n(t, 0) = (1 + \alpha) n(t, T). \quad (\text{A4})$$

**2. Full model**

Having satisfied the growth condition, we will now calculate the values of  $k_-(a)$  and  $k_+(a)$ , which represent the movement of cells between compartments. In our model, cells cannot reenter the niche compartment, so  $k_+(a) = 0$ . For expressing  $k_-(a)$ , we realize that the fixed size of the niche compartment means that for every cell division, one random cell must be removed from the niche compartment and added to the differentiation compartment. Therefore,  $k_-(a)$  is equal to the number of cells dividing in a given time interval, multiplied by the chance that a cell being ejected is a dividing cell, multiplied by the probability that the ejected cell has the age  $(a, a + da)$ :

$$k_-(a)da dt = \left[ \frac{dt}{da} n(t, T) da \right] \left( \frac{N(t)}{S} \right) \left( \frac{n(t, a) da}{N(t)} \right).$$

Here, we remind the reader that  $N(t)$  is defined as the total number of proliferating cells in the niche at time  $t$ , and that  $n(t, a)$  is the number of proliferating cells in the niche compartment of age  $a$  at time  $t$ . From this equation, it directly follows that

$$k_-(a) = \frac{n(t, T)}{S} n(t, a).$$

Inserting these results in Eq. (A1), we obtain Eq. (1):

$$\frac{\partial n(t, a)}{\partial t} + \frac{\partial n(t, a)}{\partial a} = -\frac{n(t, T)}{S} n(t, a).$$

The number of newly born proliferating cells in the niche was already defined by Eq. (A4).

For the differentiation compartment, a similar analysis can be made, noting that here  $k_-(a)$  is now negative, and  $k_+(a)$  is now equal to  $k_-(a)$  of the niche compartment. The number of proliferating cells in the differentiating compartment of age  $a$  at time  $t$  is defined as  $m(t, a)$ ,

$$\frac{\partial m(t, a)}{\partial t} + \frac{\partial m(t, a)}{\partial a} = \frac{n(t, T)}{S} n(t, a). \tag{A5}$$

The equivalent of Eq. (A4) for the differentiation compartment simply becomes

$$m(t, 0) = (1 + \alpha_m) m(t, T). \tag{A6}$$

**3. Steady state for the niche compartment**

To solve the number of proliferating cells, we assume that the age distribution is exponential,

$$n(t, a) = f(t) e^{ra}. \tag{A7}$$

Here,  $f(t)$  is a function independent of  $a$  and  $r$  is a coefficient. At  $a = 0$ , we obtain  $n(t, a = 0) = f(t)$ . From Eq. (A4), we obtain  $n(t, a = 0) = (1 + \alpha_n) n(t, T) = (1 + \alpha_n) f(t) e^{rT}$ , where we inserted Eq. (A7). This results in

$$r = -\frac{\ln(1 + \alpha_n)}{T}. \tag{A8}$$

Next, we substitute Eq. (A7) into Eq. (1),

$$\frac{\partial f(t)}{\partial t} e^{ra} + r f(t) e^{ra} = -\frac{f(t) e^{rT}}{S} f(t) e^{ra}.$$

By dividing by  $e^{ra}$  and rearranging, we find

$$\frac{\partial f(t)}{\partial t} = f(t) \left( \frac{\ln(1 + \alpha_n)}{T} - \frac{f(t)}{(1 + \alpha_n)S} \right). \tag{A9}$$

In the steady state,  $f' = f(t)$  so that  $\frac{\partial f(t)}{\partial t} = 0$ . Therefore, from Eq. (A9), two solutions arise. The first is the trivial solution  $f' = 0$ , and the second is

$$f' = (1 + \alpha_n) \frac{\ln(1 + \alpha_n)}{T} S.$$

Inserting this solution into Eq. (A7) [with Eq. (A8)] results in

$$n'(a) = (1 + \alpha_n) \frac{\ln(1 + \alpha_n)}{T} S e^{-\frac{\ln(1 + \alpha_n)}{T} a}. \tag{A10}$$

Integrating over all values of  $a$  results in the number of dividing cells in the niche compartment,

$$\begin{aligned} N' &= \int_0^T da n'(a) \\ &= (1 + \alpha_n) S \left( 1 - \frac{1}{1 + \alpha_n} \right) \\ &= \alpha_n S. \end{aligned} \tag{A11}$$

Here, we used

$$\int_0^T da e^{-\frac{\ln(1 + \alpha_n)}{T} a} = -\frac{T}{\ln(1 + \alpha_n)} (e^{-\ln(1 + \alpha_n)} - 1).$$

**4. Steady state for the differentiation compartment**

To obtain the total number of dividing cells, we also need to calculate the number of cells in the differentiation compartment. For this compartment, we need to take into account that there is an incoming supply of dividing cells from the niche compartment. In the steady state,  $\frac{\partial m(t, a)}{\partial t} = 0$ . To ensure homeostasis in the full system,  $\frac{\partial m'(a)}{\partial a} = -\frac{\partial n'(a)}{\partial a}$ . From Eq. (A10), we therefore obtain

$$\frac{\partial m'(a)}{\partial a} = (1 + \alpha_n) \left( \frac{\ln(1 + \alpha_n)}{T} \right)^2 S e^{-\frac{\ln(1 + \alpha_n)}{T} a}.$$

As the age distribution is exponential, we can state

$$m'(a) = A e^{Ba} + C.$$

From inserting this equation into the one above it and comparing terms, it follows that  $B = -\frac{\ln(1 + \alpha_n)}{T}$  and  $A = -(1 + \alpha_n) \frac{\ln(1 + \alpha_n)}{T} S$ .

From Eq. (A6), we obtain  $m'(0) = (1 + \alpha_m) m'(T)$ , resulting in

$$C = \frac{\ln(1 + \alpha_n)}{T} S \frac{\alpha_m - \alpha_n}{\alpha_m}.$$

Together,

$$m'(a) = \frac{\ln(1 + \alpha_n)}{T} S \left( \frac{\alpha_m - \alpha_n}{\alpha_m} - (1 + \alpha_n) e^{-\frac{\ln(1 + \alpha_n)}{T} a} \right).$$

With  $M' = \int_0^T da m'(a)$ , we obtain

$$M' = \ln(1 + \alpha_n) S \frac{\alpha_m - \alpha_n}{\alpha_m} - \alpha_n S.$$

With  $D = M' + N'$  and the insertion of Eq. (A11), we obtain the final result,

$$D = \ln(1 + \alpha_n) S \frac{\alpha_m - \alpha_n}{\alpha_m}.$$

This equation has solutions for  $D > 0$  if  $\alpha_m < 0$  and  $\alpha_n > 0$ . If  $\alpha_n < 0$ , then  $N'$  would be negative, and if  $\alpha_m > 0$ , then  $M'$  would be negative, both of which are not allowed.

- 
- [1] N. McCarthy, J. Kraiczky, and R. A. Shivdasani, Cellular and molecular architecture of the intestinal stem cell niche, *Nat. Cell Biol.* **22**, 1033 (2020).
- [2] S. D. C. Weterings, M. J. van Oostrom, and K. F. Sonnen, Building bridges between fields: Bringing together development and homeostasis, *Development* **148**, dev193268 (2021).
- [3] B. D. Simons and H. Clevers, Strategies for homeostatic stem cell self-renewal in adult tissues, *Cell* **145**, 851 (2011).
- [4] A. Jilkine, Mathematical models of stem cell differentiation and dedifferentiation, *Curr. Stem Cell Rep.* **5**, 66 (2019).
- [5] L. Chatzeli and B. D. Simons, Tracing the dynamics of stem cell fate, *Cold Spring Harbor Perspect. Biol.* **12**, a036202 (2020).
- [6] A. M. Klein and B. D. Simons, Universal patterns of stem cell fate in cycling adult tissues, *Development* **138**, 3103 (2011).
- [7] Y. Kitadate, D. J. Jörg, M. Tokue, A. Maruyama, R. Ichikawa, S. Tsuchiya, E. Segi-Nishida, T. Nakagawa, A. Uchida, C. Kimura-Yoshida, S. Mizuno, F. Sugiyama, T. Azami, M. Ema, C. Noda, S. Kobayashi, I. Matsuo, Y. Kanai, T. Nagasawa, Y. Sugimoto *et al.*, Competition for mitogens regulates spermatogenic stem cell homeostasis in an open niche, *Cell Stem Cell* **24**, 79 (2019).
- [8] E. Clayton, D. P. Doupe, A. M. Klein, D. J. Winton, B. D. Simons, and P. H. Jones, A single type of progenitor cell maintains normal epidermis, *Nature (London)* **446**, 185 (2007).
- [9] C. Lopez-Garcia, A. M. Klein, B. D. Simons, and D. J. Winton, Intestinal stem cell replacement follows a pattern of neutral drift, *Science* **330**, 822 (2010).
- [10] H. J. Snippert, L. G. van der Flier, T. Sato, J. H. van Es, M. van den Born, C. Kroon-Veenboer, N. Barker, A. M. Klein, J. van Rheenen, B. D. Simons, and H. Clevers, Intestinal crypt homeostasis results from neutral competition between symmetrically dividing Lgr5 stem cells, *Cell* **143**, 134 (2010).
- [11] L. Ritsma, S. I. Ellenbroek, A. Zomer, H. J. Snippert, F. J. De Sauvage, B. D. Simons, H. C. Clevers, and J. Van Rheenen, Intestinal crypt homeostasis revealed at single-stem-cell level by *in vivo* live imaging, *Nature (London)* **507**, 362 (2014).
- [12] H. Gehart and H. Clevers, Tales from the crypt: New insights into intestinal stem cells, *Nat. Rev. Gastroenterol. Hepatol.* **16**, 19 (2019).
- [13] A. M. Klein, D. P. Doupe, P. H. Jones, and B. D. Simons, Kinetics of cell division in epidermal maintenance, *Phys. Rev. E* **76**, 021910 (2007).
- [14] Z. Sun and N. L. Komarova, Stochastic modeling of stem-cell dynamics with control, *Math. Biosci.* **240**, 231 (2012).
- [15] B. Corominas-Murtra, C. L. Scheele, K. Kishi, S. I. Ellenbroek, B. D. Simons, J. Van Rheenen, and E. Hannezo, Stem cell lineage survival as a noisy competition for niche access, *Proc. Natl. Acad. Sci. USA* **117**, 16969 (2020).
- [16] V. L. Cannataro, S. A. McKinley, and C. M. St. Mary, The implications of small stem cell niche sizes and the distribution of fitness effects of new mutations in aging and tumorigenesis, *Evol. Appl.* **9**, 565 (2016).
- [17] V. L. Cannataro, S. A. McKinley, and C. M. St. Mary, The evolutionary trade-off between stem cell niche size, aging, and tumorigenesis, *Evol. Appl.* **10**, 590 (2017).
- [18] L. Shahriyari and N. L. Komarova, The role of the bi-compartmental stem cell niche in delaying cancer, *Phys. Biol.* **12**, 055001 (2015).
- [19] Y. Sei, J. Feng, C. C. Chow, and S. A. Wank, Asymmetric cell division-dominant neutral drift model for normal intestinal stem cell homeostasis, *Am. J. Physiol. Gastrointest. Liver Physiol.* **316**, G64 (2019).
- [20] J. Yang, M. V. Plikus, and N. L. Komarova, The role of symmetric stem cell divisions in tissue homeostasis, *PLoS Comput. Biol.* **11**, e1004629 (2015).
- [21] A. Azzalini and A. Capitanio, Statistical applications of the multivariate skew normal distribution, *J. R. Stat. Soc. Ser. B* **61**, 579 (1999).
- [22] G. Huelsz-Prince, R. N. U. Kok, Y. J. Goos, L. Bruens, X. Zheng, S. I. Ellenbroek, J. van Rheenen, S. J. Tans, and J. S. van Zon, Mother cells control daughter cell proliferation in intestinal organoids to minimize proliferation fluctuations, *eLife* **11**, e80682 (2022).
- [23] M. Inaba and Y. M. Yamashita, Asymmetric stem cell division: Precision for robustness, *Cell Stem Cell* **11**, 461 (2012).
- [24] Z. G. Venkei and Y. M. Yamashita, Emerging mechanisms of asymmetric stem cell division, *J. Cell Biol.* **217**, 3785 (2018).
- [25] C. S. Baron and A. van Oudenaarden, Unravelling cellular relationships during development and regeneration using genetic lineage tracing, *Nat. Rev. Mol. Cell Biol.* **20**, 753 (2019).
- [26] A. McKenna and J. A. Gagnon, Recording development with single cell dynamic lineage tracing, *Development* **146**, dev169730 (2019).
- [27] L. Li and T. Xie, Stem cell niche: Structure and function, *Annu. Rev. Cell Dev. Biol.* **21**, 605 (2005).